
Mechanics of woven fabrics using cruciform elements

Raj Ramgulam — Prasad Potluri

*School of Materials
The University of Manchester
Textiles & Paper, Sackville Street
Manchester
M60 1QD*

*R.Ramgulam@manchester.ac.uk
Prasad.Potluri@manchester.ac.uk*

ABSTRACT. This paper presents a cruciform element for finite element modelling of woven fabrics. Unlike shell elements, cruciform elements do not need special forms near curved boundaries. Additionally, cruciform elements represent the discrete nature of textile structures and ensure that the arms of the cruciform are parallel to the warp and weft directions. In this paper, stiffness matrices for three types of loading, biaxial tensile, in-plane shear and in-plane bending, have been derived. FE modelling with cruciform elements has been demonstrated for bias extension of a woven fabric near the fixed clamp region.

KEYWORDS: woven fabric, cruciform, draping, forming, tensile, shear.

1. Introduction

Stress-strain relationships for a woven cloth were developed by approximating the cloth as a simple trellis in which the elements do not pass under and over each other (Kilby, 1963). To account for the Poisson effect in actual fabrics he assumed that a woven cloth is equivalent to an anisotropic lamina that exhibits Poisson effect. He obtained a very useful relationship for the extensional modulus of a fabric in different directions as well as an approximate relationship between fabric modulus in any direction and shear modulus.

Lloyd proposed a detailed finite-element analysis of complex fabric deformations with the aid of shell elements (Lloyd, 1980) that dealt with small strain and linear elastic deformations. He extended this to include non-linear material properties, large strains and large deformations. A finite element method was used for calculating the shape of sails and other inflated fabric structures (Torbe, 1975). In this work, Torbe proposed a cruciform element specifically suited to textiles. This element approximates a fabric not as a continuous membrane but as a coarser representative grid than that is formed by yarns. Another interesting paper deals with draping by treating a fabric as a membrane (Williams, 1984). His approach makes an extensive use of differential geometry.

Collier *et al.*, considered fabrics as an orthotropic shell for FEM analysis in order to predict the draping behaviour under gravity loading (Collier *et al.*, 1991). They classify the problem as one involving large deformations with small strain. The non-linearity due to changes in geometry is accounted for by a sequence of linear problems through incrementing the applied load. The stiffness matrix, as a function of displacements, is calculated at each step. While the clothing and entertainment industries have been interested in gravity drape problems, the composites industry has been looking at contact drape problems to simulate the fitting of textile preforms on mould surfaces under membrane loads. The fishnet algorithm is the starting point for obtaining the initial geometric configuration (Van West *et al.*, 1990). Long *et al.* used the fishnet algorithm within an iterative procedure that minimizes the total strain energy using an optimization technique (Long *et al.*, 2000). The strain energy for shear deformation is obtained through experiments. FE software based on the commercial metal stamping code PAM-STAMP^{TM4} has also been applied for draping continuous fibre reinforced thermoplastics (CFRTP). Each ply of stacks of CFRTP is modelled separately with shell elements to capture the shear deformation in and between plies (De Luca, 1998). A fabric reinforced fluid model (Lamers *et al.*, 2001) has been developed in the finite element package DIEKA to predict fiber orientation in Rubber Press Forming process for specified boundary conditions. Finite element-based forming simulations were performed with the aid of biaxial tensile test data (Boisse *et al.*, 1997, 2000, 2001). Fabric draping can also be modelled by taking into account the mechanical properties of the cloth through springs and masses (Boubaker *et al.*, 2002), representing the tensile and torsional properties of the cloth. The equilibrium shape is obtained by minimizing the potential energy of the system using the Lagrange multiplier method. Another FE

based fabric draping model uses the fishnet model to obtain an initial solution (Sharma *et al.*, 2003). A mesh is then generated on the deformed section and an FE analysis performed assuming the material as a membrane. This process is repeated until the whole fabric has been draped. More recently the same authors (Sharma *et al.*, 2004) described an FE approach that modelled a fabric as a network of simple truss elements, connected across the diagonals by soft elements to mimic the shear stiffness of the material.

In this paper, we introduce a cruciform element for forming simulations. The cruciform element, originally developed by (Torbe, 1975) for biaxial tension and shear, has been extended to include in-plane yarn bending. Often ignored in forming simulations, in-plane yarn bending is an important mechanism for explaining the transition from no shear to maximum shear near fixed clamp regions (such as blank holders).

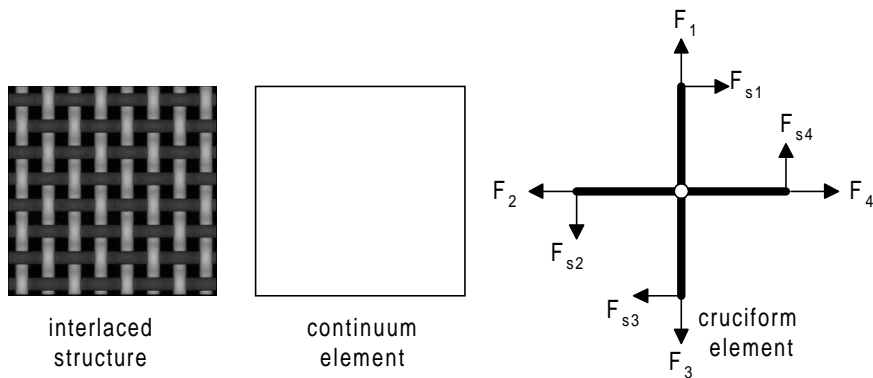


Figure 1. *Cruciform element*

2. Cruciform element

FE based forming simulations treat the fabric as a continuum and divide the surface into 2D shell or membrane elements (figure 1). Constitutive material properties are obtained experimentally using biaxial tensile and picture-frame test rigs. Alternately, constitutive properties can be predicted with the help of meso-scale models (Ramgulam *et al.*, 2004) and subsequently homogenised for continuum. Since the fabric is itself a mesh, the use of continuous membrane may not be necessary (Torbe, 1975). A cruciform element, Figure 1, adequately represents the fabric structure. Moreover, no special form of the element is needed to accommodate curved surfaces or different types of boundaries. The nodes of the cruciform are the ends of the four arms while the crossover point is a hinge and not a node (except when modelling bending). The cruciform element is considered superior to the more commonly used continuum element to model the mechanical behaviour of woven fabrics under different conditions including the draping process. As such a pair of rods pin-jointed will not be capable of representing biaxial load

deformation of woven fabrics characterised by Poisson transverse strain effects nor will such a structure represent shear resistance. However it is required to define the actual characteristics of the material and incorporate these in the FE model. Three important deformation characteristics are used to describe the mechanics of woven cloths: bending with the hinge assumed to be fixed joint, shear resistance mainly due to friction between the yarns and biaxial fabric deformation. Nodal forces can be resolved into axial forces (F_1, F_2, F_3, F_4) responsible for biaxial tensile deformations and transverse forces ($F_{s1}, F_{s2}, F_{s3}, F_{s4}$) responsible for shear and yarn bending (figure 1).

3. FE model of biaxial loading deformation

Consider the cruciform element in Figure 2 representing a rectangular part of a fabric under biaxial loading.

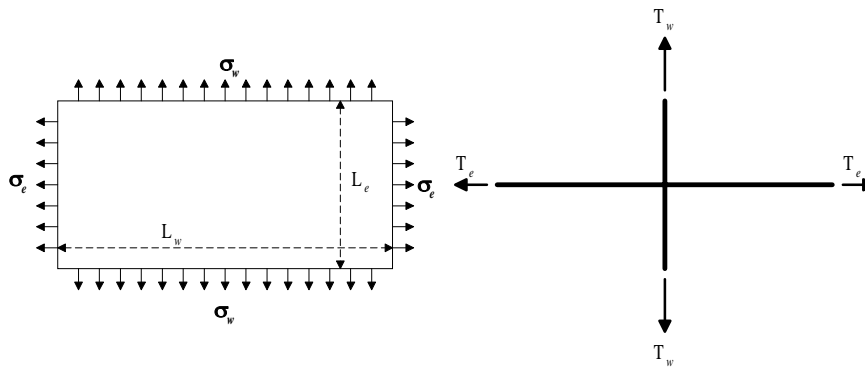


Figure 2. Loads on continuum and cruciform elements

$$\varepsilon_w = \frac{\sigma_w}{E_w} - \frac{\nu_e \cdot \sigma_e}{E_e} \quad \varepsilon_e = \frac{\sigma_e}{E_e} - \frac{\nu_w \cdot \sigma_w}{E_w} \quad [1]$$

where,

ε_w and ε_e are strains, σ_w and σ_e are stresses (defined as load per unit width), ν_w and ν_e are Poisson's ratio and E_w and E_e are the extensional moduli in the warp and weft directions respectively.

Re-writing the equation [1] in terms of stresses,

$$\sigma_w = E_w(\varepsilon_w + \mu_e \cdot \varepsilon_e) \quad \sigma_e = E_e(\varepsilon_e + \mu_w \cdot \varepsilon_w) \quad [2]$$

where,

$$\mu_w = \frac{\nu_w}{1 - \nu_w \nu_e} \quad \mu_e = \frac{\nu_e}{1 - \nu_w \nu_e} \quad [3]$$

For the cruciform element, $T_w = \sigma_w \cdot L_e$ $T_e = \sigma_e \cdot L_w$ and hence,

$$T_w = k_w (\epsilon_w + \mu_e \cdot \epsilon_e) \quad T_e = k_e (\epsilon_e + \mu_w \cdot \epsilon_w) \quad [4]$$

where,

$$k_w = L_e \cdot E_w \quad k_e = L_w \cdot E_e \quad [5]$$

Element stiffness matrix

The following analysis refers to figure 3 which depicts a general cruciform element on published work for inflated structures (Torbe, 1975). T_i and a_i are the tension and length of the arms of the cruciform, where $i = 1$ to 4.

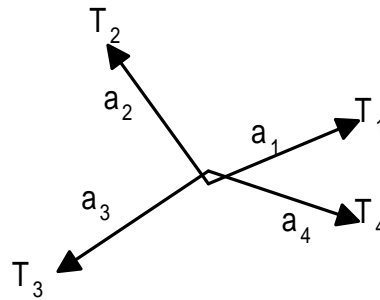


Figure 3. General cruciform element

Given that u_i and v_i represent displacement at the nodes and u_o and v_o at the hinge or crossover point:

$$U^T = [u_1 \quad v_1 \quad u_2 \quad v_2 \quad u_3 \quad v_3 \quad u_4 \quad v_4] \quad U_0^T = [u_0 \quad v_0]$$

$$\Gamma^T = [\epsilon_1 \quad \epsilon_2 \quad \epsilon_3 \quad \epsilon_4] \quad D^T = \begin{bmatrix} l_1 & l_2 & l_3 & l_4 \\ m_1 & m_2 & m_3 & m_4 \end{bmatrix}$$

$$C = \begin{bmatrix} 1/a_1 & 0 & 0 & 0 \\ 0 & 1/a_2 & 0 & 0 \\ 0 & 0 & 1/a_3 & 0 \\ 0 & 0 & 0 & 1/a_4 \end{bmatrix} \quad \Omega = \begin{bmatrix} l_1 & m_1 & 0 & 0 & 0 & 0 & 0 & 0 \\ 0 & 0 & l_2 & m_2 & 0 & 0 & 0 & 0 \\ 0 & 0 & 0 & 0 & l_3 & m_3 & 0 & 0 \\ 0 & 0 & 0 & 0 & 0 & 0 & l_4 & m_4 \end{bmatrix}$$

where a_i are the lengths of the arms of the element and l_i and m_i are the direction cosines of element's arms.

In the case of a square element (used in section 6) following relationship holds:

$$a_1 = a_2 = a_3 = a_4 = L$$

$$\text{In that case } C = \frac{1}{L} \begin{bmatrix} 1 & 0 & 0 & 0 \\ 0 & 1 & 0 & 0 \\ 0 & 0 & 1 & 0 \\ 0 & 0 & 0 & 1 \end{bmatrix}$$

$$\text{For small deformations: } \varepsilon_i = \frac{l_i(u_i - u_0)}{a_i} + \frac{m_i(v_i - v_0)}{a_i} \quad [6]$$

$$\text{In matrix notation strain is given as follows: } \Gamma = C.\Omega.U - C.D.U_0 \quad [7]$$

The yarn tensions, T , are expressed in terms of strains by $T = K.\Gamma$, given more explicitly as follows:

$$\begin{bmatrix} T_1 \\ T_2 \\ T_3 \\ T_4 \end{bmatrix} = \begin{bmatrix} k_1 & \alpha_1 & 0 & \alpha_1 \\ \alpha_2 & k_2 & \alpha_2 & 0 \\ 0 & \alpha_1 & k_1 & \alpha_1 \\ \alpha_2 & 0 & \alpha_2 & k_2 \end{bmatrix} \begin{bmatrix} \varepsilon_1 \\ \varepsilon_2 \\ \varepsilon_3 \\ \varepsilon_4 \end{bmatrix} \quad [8]$$

where,

$$k_1 = (a_2 + a_4)E_w \quad k_2 = (a_1 + a_3)E_e$$

$$\alpha_1 = \frac{k_1\mu_e}{2} \quad \alpha_2 = \frac{k_2\mu_w}{2}$$

Given equilibrium conditions at crossover point, i.e. resultant force=0:

$$D^T.K.\Gamma = 0 \quad [9]$$

Combining equations 7 and 9:

$$D^T . K . \Gamma = D^T . K . C . \Omega U - D^T . K . C . D U_0 \quad [10]$$

Hence:

$$D^T . K . C . \Omega U = D^T . K . C . D U_0 \quad [11]$$

Let $\Psi = D^T . K . C . D$

Rewriting equation 11 gives:

$$U_0 = \Psi^{-1} . D^T . K . C . \Omega U \quad [12]$$

Therefore rewriting equation 7 gives

$$\begin{aligned} \Gamma &= C . \Omega U - C . D . \Psi^{-1} . D^T . K . C . \Omega U \\ &= (I - C . D . \Psi^{-1} . D^T . K) . (C . \Omega) U \end{aligned} \quad [13]$$

$$F = -L^T . K . \Gamma = -\Omega^T . K . (I - C . D . \Psi^{-1} . D^T . K) . (C . \Omega) U \quad [14]$$

where F is the vector of nodal force components.

Hence

$$\text{Stiffness Matrix} = -\Omega^T . K . (I - C . D . \Psi^{-1} . D^T . K) . (C . \Omega) \quad [15]$$

Stiffness matrix is depending on the geometry of the cruciform element and fabric properties.

4. Finite element model for shear

Shear deformation on a cloth element is illustrated in Figure 4. The cruciform element is shown embedded in the unit. The fabric shear property, characterised as shear stiffness G (N/cm), is obtained experimentally. The cloth element (and hence the cruciform) deforms by an angle γ with the application of shear stress τ .

Shear Stress in N/cm: $\tau = G . \gamma$

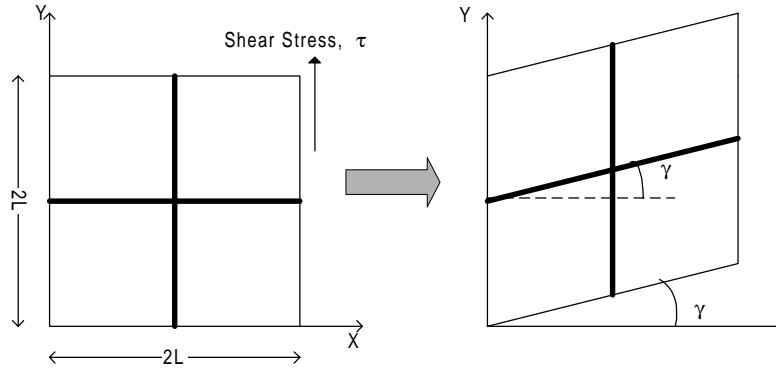


Figure 4. Shear deformation

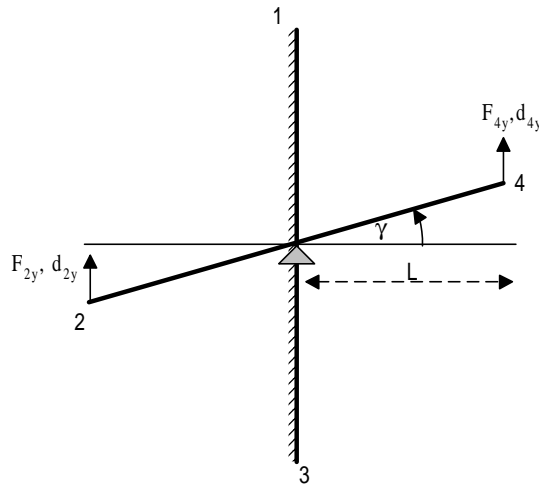


Figure 5. Element for shear deformation model

A simple element stiffness matrix has been constructed for small shear deformations. In this case the element, Figure 5, is assumed to rotate at its centre. For the two node element, Figure 5, displacements, d_{2y} and d_{4y} are given in the element coordinate system with x-axis along the beam axis and the y-axis is vertical. The loads applied to the element are F_{2y} and F_{4y} . Referring to figure 4 and figure 5,

$$\text{StrainEnergy} = U = \frac{1}{2} G \frac{(d_{4y} - d_{2y})^2}{4L^2} .A \quad [16]$$

where G is the shear modulus and A is the area of the unit cell.

$$\text{PotentialEnergy} = -F_{2y} \cdot d_{2y} - F_{4y} \cdot d_{4y} \quad [17]$$

$$\Pi = \text{StrainEnergy} + \text{PotentialEnergy}$$

$$\frac{\partial \Pi}{\partial d_{2y}} = -\frac{AG}{4L^2}(d_{4y} - d_{2y}) - F_{2y} \quad [18]$$

$$\frac{\partial \Pi}{\partial d_{4y}} = \frac{AG}{4L^2}(d_{4y} - d_{2y}) - F_{4y} \quad [19]$$

$$\text{Hence, } \begin{bmatrix} F_{2y} \\ F_{4y} \end{bmatrix} = \frac{AG}{4L^2} \begin{bmatrix} 1 & -1 \\ -1 & 1 \end{bmatrix} \begin{bmatrix} d_{2y} \\ d_{4y} \end{bmatrix} \quad [20]$$

The element stiffness matrix in terms of global coordinates is

$$K_s = Q_s^T k_s^g Q_s \quad [21]$$

where,

$$Q_s = \begin{bmatrix} l & m & 0 & 0 \\ -m & l & 0 & 0 \\ 0 & 0 & l & m \\ 0 & 0 & -m & l \end{bmatrix} \text{ and } k_s^g = \frac{AG}{4L^2} \begin{bmatrix} 0 & 0 & 0 & 0 \\ 0 & 1 & 0 & -1 \\ 0 & 0 & 0 & 0 \\ 0 & -1 & 0 & 1 \end{bmatrix} \quad [22]$$

5. Finite element model for bending

Figure 6 illustrates the importance of yarn bending. If the yarn bending is ignored, the deformation cannot propagate from a fixed clamp to maximum shear region (one can easily verify this behaviour with the help of a garden trellis). Flexural rigidity of each arm of a cruciform element is the sum of the flexural rigidity of the warp or weft yarns (with in the area of the element).

$$E_b I = (E_b I)_y \cdot n \cdot 2L \quad [23]$$

where,

$E_b I$ is the flexural rigidity of the cruciform, $(E_b I)_y$ is the flexural rigidity of a yarn and n is the number of warp/weft yarns per unit length. If the warp and weft

densities are not identical, equation [23] must be evaluated for warp and weft separately.

A cubic displacement function with 4 coefficients (λ_i) is chosen given that the exact solution of the beam bending problem with only concentrated loads is a piecewise continuous cubic polynomial with first derivative continuity.

$$d = \lambda_1 x^3 + \lambda_2 x^2 + \lambda_3 x + \lambda_4 \quad [24]$$

where d is the displacement for different values of x measured along the element.

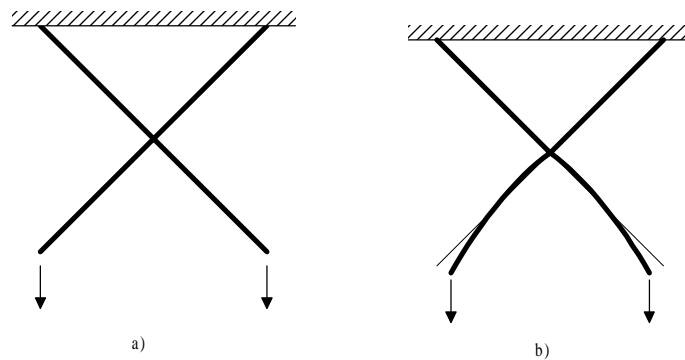


Figure 6. a) no yarn bending, b) yarn bending

Figure 7 shows a three node beam element representing one arm of the cruciform element. In the present analysis, both the arms are assumed to be identical representing a case of equal warp and weft densities. F_{iy} , d_{iy} , m_i and ϕ_i represent nodal forces, nodal displacements, moments and angles for $i=1$ to 3.

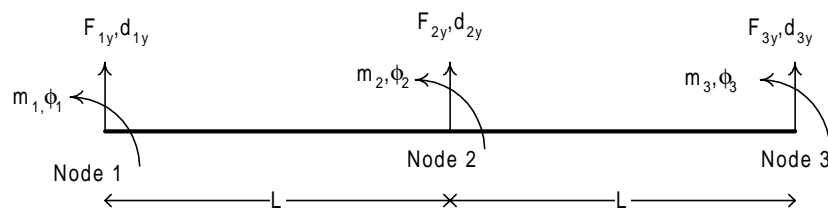


Figure 7. Three node element for bending

Node 2 is situated at the hinge joint of a cruciform element. At node 2, displacements are not allowed. Using the principle of minimum energy the element stiffness matrix for the 3-node element has been derived as:

$$k_{b3} = \frac{E_b I}{L^3} \begin{bmatrix} 12 & 6L & 6L & 0 & 0 \\ 6L & 4L^2 & 3L^2 & 0 & 0 \\ 6L & 3L^2 & 8L^2 & -6L & 2L^2 \\ 0 & 0 & -6L & 12 & -6L \\ 0 & 0 & 2L^2 & -6L & 4L^2 \end{bmatrix} \quad [25]$$

Stiffness matrix in terms of global coordinates is

$$K_b = Q^T \cdot k_{b3}^g \cdot Q \quad [26]$$

where,

$$Q = \begin{bmatrix} l & m & 0 & 0 & 0 & 0 & 0 \\ -m & l & 0 & 0 & 0 & 0 & 0 \\ 0 & 0 & 1 & 0 & 0 & 0 & 0 \\ 0 & 0 & 0 & 1 & 0 & 0 & 0 \\ 0 & 0 & 0 & 0 & m & l & 0 \\ 0 & 0 & 0 & 0 & -l & m & 0 \\ 0 & 0 & 0 & 0 & 0 & 0 & 1 \end{bmatrix} \quad [27]$$

$$k_{b3}^g = \frac{E_b I}{L^3} \begin{bmatrix} 0 & 0 & 0 & 0 & 0 & 0 & 0 \\ 0 & 12 & 6L & 6L & 0 & 0 & 0 \\ 0 & 6L & 4L^2 & 3L^2 & 0 & 0 & 0 \\ 0 & 6L & 3L^2 & 8L^2 & 0 & -6L & 2L^2 \\ 0 & 0 & 0 & 0 & 0 & 0 & 0 \\ 0 & 0 & 0 & -6L & 0 & 12 & -6L \\ 0 & 0 & 0 & 2L^2 & 0 & -6L & 4L^2 \end{bmatrix} \quad [28]$$

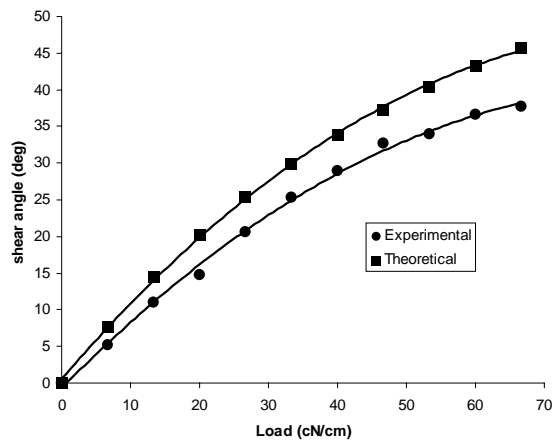
6. Experimental validation

A fabric with characteristics shown in Table 1 has been used for experimental work. A 7.5 cm wide and 22 cm long sample was prepared by cutting the fabric along the bias direction. The sample was clamped at one end and load applied at the other end to simulate a bias extension test. Figure 9a shows half of the fabric sample, with fixed boundaries on one side. A flatbed scanner was used to capture the image of the fabric under different loadings. The images were then analysed for computing the shear angles.

Table 1. *Fabric specifications*

Fabric	Yarn	Filament
Structure: Plain Weave	Linear density: 1200 Tex	Type: E Glass
Ends/cm: 2.4	Number of filaments: 2000	Modulus: 72.4 GPa
Picks/cm: 2.4	Flexural Rigidity: 0.6 Nmm ²	Density: 2.5g/cm ³
Shear Modulus: 0.96 N/cm		Diameter: 17 μ m
E_w, E_e : 520 N/cm		
ν_w, ν_e : 0.45		

Finite element simulations were performed with 59 cruciform elements representing a fabric area of 2.4 cm x 3.6 cm. FE model shown in figure 9b represents one half of a bias test, from the fixed end to the centre. All the element equations for each mode of deformation were assembled to form 3 separate systems of linear equations. Gauss elimination was used to solve each set of equations to give the nodal displacement resulting from tensile, bending and shear deformations successively. Figure 8 compares experimental data with simulation results; FE predictions are about 15% higher than the experimental shear angles. The thin lines, in Figure 9b, represent the centerlines of yarns in the un-deformed fabric while the thicker superimposed lines represent the deformed yarns. Figure 9b clearly shows that the yarn bending results in the progression from no shear near the clamped region to maximum shear.

**Figure 8.** *Shear angle versus bias load*

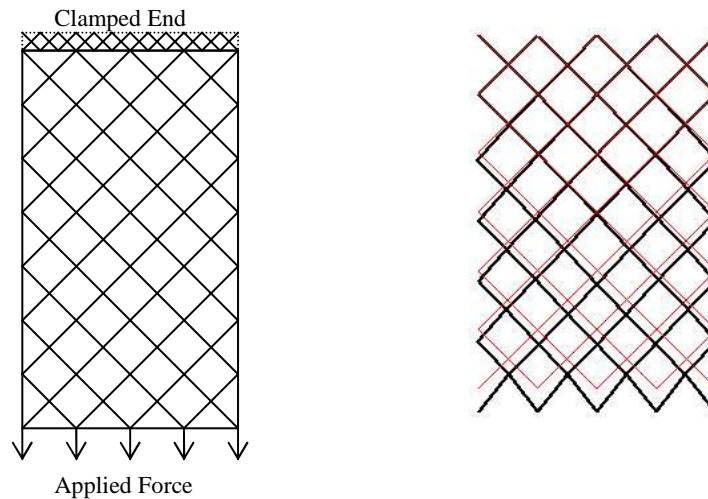


Figure 9. a) Fabric test setup

b) Deformed fabric- FE simulation

7. Discussion

Finite element modelling of woven fabrics has been demonstrated with the aid of cruciform elements as opposed to conventional shell or membrane elements. The model is currently valid for small deformations-shear model needs further improvement to account for large deformations. The use of the cruciform element though adding to the complexity of overall methodology has distinct advantages over the continuous type element given the special highly directional characteristics of woven fabrics. In future, cruciform-based FE modelling will be extended to 3D forming simulations.

8. References

- Boisse P., Borr M., Buet K., Cherouat A., "Finite element simulations of textile composite forming including the biaxial fabric behaviour", *Composites Part B*, Vol. 28B, 1997, pp. 453-464.
- Boisse P., Daniel J., Gasser A., Hivet G., Soulat D., "Prise en compte du procédé de fabrication dans la conception des structures composites minces", *Mécanique & Industries*, Vol. 1, 2000, pp. 303-311.
- Boisse P., Gasser A., Hivet G., "Analyses of fabric tensile behaviour: determination of the biaxial tension-strain surfaces and their use in forming simulations", *Composites Part A*, Vol. 32, 2001, pp. 395-1414.
- Boubaker B.B., Haussy B., Ganghoffer J., Modèles discrets de tissus tissées: Analyse de stabilité et de drapé, *Comptes Rendus Mécanique*, Vol. 330, 2002, pp. 871-877.

- Chicurel R., Suppiger E., "Load-deflection analysis of fibers with plane crimp", *Textile Research Journal*, 1960, pp. 568-575.
- Collier J.R., Collier B.J., O'Toole G., Sargand S.M., "Drape prediction by means of finite element analysis", *Journal of the Textile Institute*, Vol. 82, No. 1, 1991, pp. 96-102.
- De Luca P., Lefébure P., Pickett A.K., "Numerical and experimental investigation of some press forming parameters of two fibre reinforced thermoplastics: APC2-AS4 and PEI-CETEX", *Composites Part A*, Vol. 29A, 1998, pp. 101-110.
- Kilby W.F., "Planar stress-strain relationships in woven fabrics", *Journal of the Textile Institute*, Vol. 55, 1963, pp. 9-27.
- Lamers E.A.D., Wijsskamp S., Akkerman R., "Modelling of fabric draping: Finite elements versus geometrical method", *4th ESAFORM Conference on Material Forming*, Liège, 2001.
- Long A.C., Souter B.J., Robitaille F., "A fabric mechanics approach to draping of woven and non-crimp reinforcements", *Proc. 15th Annual Technical Conf., American Society for Composites*, Texas A&M University, USA, September 2000, pp. 76-83.
- Lloyd D.W., "The analysis of complex fabric deformations", *Mechanics of flexible fibre assemblies, NATO Advanced Study Institute Series*, Sijthoff & Noordhoff, 1980, pp. 311-341.
- Ramgulam R., Potluri P., "Tensile load deformation behaviour of woven Fabrics", *Proceedings of 2004 ASME: International Mechanical Engineering Congress and R&D Expo*, November 13-19, 2004, Anaheim, Ca.
- Sharma S.B., Sutcliffe M.P.F., "Draping of woven fabrics: Progressive drape model", *Plastics Rubber and Composites*, Vol. 32, 2003, pp. 57-64.
- Sharma S.B., Sutcliffe M.P.F., "A simplified finite element model for draping of woven material", *Composites Part A*, Vol. 35, 2004, pp. 647-643.
- Torbe I., "A cruciform element for the analysis of fabric structures", *Proceedings of Institute of Mathematics, Conference on Finite Element Methods*, Brunel University, 1975, London, pp. 359-367.
- Van West B.P., Pipes R.B., Keefe M., "A simulation of the draping of bi-directional fabrics over arbitrary surfaces", *Journal of the Textile Institute*, Vol. 81, No. 4, 1990, pp. 448-460.
- Williams C.J.K., "Defining and designing curved flexible tensile surface structures", *The Institute of Math and its Application Conference Series*, University of Manchester, 1984.